Quantum Spin Liquid in Frustrated One-Dimensional LiCuSbO$_4$

S. E. Dutton,[1,*] M. Kumar,[1] M. Mourigal,[2,3] Z. G. Soos,[1] J.-J. Wen,[2] C. L. Broholm,[2] N. H. Andersen,[4]
Q. Huang,[5] M. Zbiri,[3] R. Toft-Petersen,[4] and R. J. Cava[1,4]

[1]*Department of Chemistry, Princeton University, Princeton, New Jersey 08544, USA*
[2]*Institute for Quantum Matter and Department of Physics and Astronomy, Johns Hopkins University,
Baltimore, Maryland 21218, USA*
[3]*Institut Laue-Langevin, BP 156, 38042 Grenoble Cedex 9, France*
[4]*Department of Physics, Risø Campus, Technical University of Denmark,
Building 228, Frederiksborgvej 399, DK-4000 Roskilde, Denmark*
[5]*Center for Neutron Research, NIST, Gaithersburg, Maryland 20899, USA*
(Received 19 September 2011; published 3 May 2012)

A quantum magnet, LiCuSbO$_4$, with chains of edge-sharing spin-$\frac{1}{2}$ CuO$_6$ octahedra is reported. While short-range order is observed for $T < 10$ K, no zero-field phase transition or spin freezing occurs down to 100 mK. Specific heat indicates a distinct high-field phase near the 12 T saturation field. Neutron scattering shows incommensurate spin correlations with $q = (0.47 \pm 0.01)\pi/a$ and places an upper limit of 70 μeV on any spin gap. Exact diagonalization of 16-spin easy-plane spin-$\frac{1}{2}$ chains with competing ferro- and antiferromagnetic interactions ($J_1 = -75$ K, $J_2 = 34$ K) accounts for the $T > 2$ K data.

The Heisenberg spin-$\frac{1}{2}$ chain is one of very few quantum critical systems to be realized in a crystalline solid. An element of frustration is added by next-nearest-neighbor interactions (J_2) [1–3]. In such systems, theoretical work [4–9] indicates that qualitatively different quantum phases are possible as a function of $\alpha = J_2/J_1$, axial exchange anisotropy Δ, and the applied field $h = g\mu_B H/|J_1|$. Finite values of α are observed in copper oxide spin chains formed by corner- or edge-sharing Jahn-Teller distorted CuO$_6$ polyhedra [10–17]. While the sign and magnitude of J_1 are dependent on the Cu-O-Cu bond angles, J_2 is always antiferromagnetic (AFM), ensuring frustration. For FM-AFM chains with ferromagnetic (FM) nearest-neighbor interactions ($J_1 < 0$), theory indicates a quantum critical point at $\alpha_c = -0.25$, $\Delta = 1$ [18,19], which separates a gapless FM state ($\alpha > \alpha_c$) from a short-range ordered (SRO) phase with a small yet finite gap ($\alpha < \alpha_c$) [20]. Dimer, spiral, vector-chiral, and multipolar phases have been predicted as a function of α, Δ, and h [4,6,8]. Interest has been further amplified by the observation that ferroelectricity accompanies magnetic ordering in some of these systems [14,21,22].

Known spin-$\frac{1}{2}$ FM-AFM chains span a wide range of α and include Li$_2$CuO$_2$ [17,21,22], SrCuO$_2$ [15], LiCuVO$_4$ [11,14,23], Li$_2$CuZrO$_4$ [10], and A_2Cu$_2$Mo$_3$O$_{12}$ ($A =$ Rb, Cs) [12,13]. With the exception of A_2Cu$_2$Mo$_3$O$_{12}$ ($A =$ Rb, Cs), all order in three dimensions (3D) and cannot be fully magnetized in Nb$_3$Sn superconducting electromagnets; the exception has a more complex structure where Dzyaloshinskii-Moriya interactions dominate the low T behavior [24].

Here we present the structure and magnetic properties of the one-dimensional (1D) spin chain compound LiCuSbO$_4$. Because of weak interchain interactions, it has no 3D ordering down to 100 mK and can be driven to a saturated-FM phase above the experimentally accessible field $\langle\mu_0 H_s\rangle = 12$ T. The magnetic susceptibility, isothermal magnetization, and specific heat can be simultaneously modeled for $T > 2$ K by using the approximate spin Hamiltonian:

$$\mathcal{H} = J_1 \sum_r \Bigg(\frac{3}{2+\Delta}(S_r^x S_{r+1}^x + S_r^y S_{r+1}^y + \Delta S_r^z S_{r+1}^z) + \alpha \mathbf{S}_r \cdot \mathbf{S}_{r+2} - h(S_r^z \cos\theta + S_r^x \sin\theta) \Bigg).$$

Here θ is the angle between the applied field h and the unique molecular axis z. The parameters $J_1 = -75$ K, $\alpha = -0.45$, and $\Delta = 0.83$ account for the main features in the thermomagnetic data and are also consistent with the magnetic excitations measured by inelastic neutron scattering.

Powder samples of LiCuSbO$_4$ were prepared by using a ceramic synthesis [25]. LiCuSbO$_4$ has an orthorhombic structure [26,27] related to that of LiFeSnO$_4$ [28]. Rietveld analysis [29] of powder neutron diffraction data acquired on the BT1 diffractometer at NIST [30] was carried out by using FULLPROF [31]. The final fit, with the corresponding crystal structure, is displayed in Fig. 1, and the structure is given in Table I. Further details of the structural refinement are given in Ref. [30]. In LiCuSbO$_4$, edge-sharing CuO$_6$ octahedra form chains along the a axis, and our analysis limits Li or Sb defect occupancy on the Cu sites to less than 1%. As expected for d^9 Cu^{2+} ions, a Jahn-Teller distortion results in significant elongation of the axial Cu-O bonds. The relatively low symmetry allows for some alternation of Cu-O bond lengths and angles
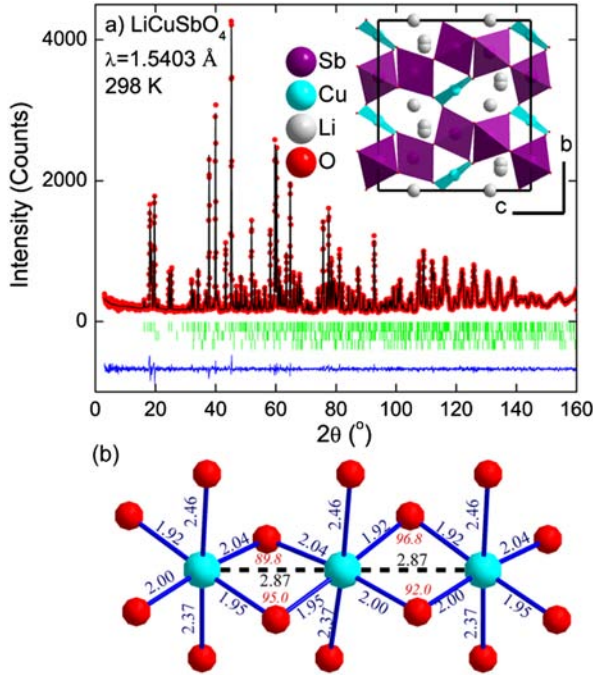
FIG. 1 (color online).   (a) Observed (red circles) and calculated
($-$) neutron diffraction data for $LiCuSbO_4$ collected at 298 K.
The difference curve is also shown; reflection positions are
indicated by the vertical lines for $LiCuSbO_4$ (upper) and the
$LiSbO_3$ [2.73(10) wt %] (middle) and CuO [0.43(5) wt %]
(lower) impurity phases. A polyhedral model looking down the
CuO_6 chains is inset. The Jahn-Teller distorted CuO_6 polyhedra
are represented with the long axial Cu-O bonds omitted. (b) Ball
and stick model showing the connectivity of the Cu chains in
$LiCuSbO_4$. Cu-Cu-and Cu-O bond lengths are black and blue,
respectively, and Cu-O-Cu bond angles are red.

along the chains [Fig. 1(b)], although only a single Cu-Cu
intrachain distance occurs. While the connectivity of the
Cu atoms within the chains is similar to that of recently
studied frustrated FM-AFM spin-$\frac{1}{2}$ chain compounds
[10–15], the easy axes of the CuO_6 octahedra in adjacent
chains are not parallel. This unique feature of $LiCuSbO_4$
may be responsible for weaker interchain interactions
which suppress 3D ordering.

Magnetization measurements on a powder sample of
$LiCuSbO_4$ were carried out by using a Quantum Design
physical properties measurement system with a 9 T magnet
and a CRYOGENIC cryogen free measurement system
with a 16 T magnet. Magnetic susceptibility ($\chi =
dM/dH$) measurements [Fig. 2(a)] were performed after
cooling in either zero field or the measuring field. In lower-
field measurements, $\mu_0 H \leq 11$ T, a broad maximum in χ,
characteristic of SRO, is observed at $T = T_m$. In applied
fields, T_m initially increases from ~ 6 K at 0.1 T to a
maximum ~ 9 K at 2 T. In higher field, a decrease in T_m
is observed [Fig. 3(c)], until, at 16 T, χ continues to
increase monotonically upon cooling, indicating a
crossover to field-induced FM. The absence of a low T
Curie tail in the SRO order regime indicates the high

TABLE I. Structural parameters for $LiCuSbO_4$ obtained from
neutron powder diffraction at 298 K, $\lambda = 1.5403$ Å. The refine-
ment was carried out in the $Cmc2_1(36)$ space group with
$a = 5.742\,60(4)$ Å, $b = 10.869\,25(7)$ Å, $c = 9.730\,48(6)$ Å,
and $V = 609.528(7)$ Å^3. The final weighted residual error R_{wp}
is 8.90. See Ref. [30] for further details.

	x	y	z	B_{iso} (Å^2)	Frac.
Sb1(4a)	0	0.3108(3)	0.2696(4)	0.13(5)	1.0
Sb2(4b)	0	0.1677(4)	$-0.0050(5)$	0.16(5)	1.0
Cu(8b)	0.7500(0)	0.410 30(15)	0.0(0)	0.49(3)	1.0
Li1a(4a)	0	0.344(2)	0.6974(13)	0.3(2)	0.5
Li1b(4a)	0	0.378(2)	0.6974(13)	0.3(2)	0.5
Li2(8b)	0.026(4)	0.0002(12)	0.2660(13)	0.5(3)	0.5
O1(4a)	0	0.0039(3)	0.0788(4)	0.45(6)	1.0
O2(4a)	0	0.3264(4)	0.9026(4)	0.37(7)	1.0
O3(4a)	0	0.4538(3)	0.1400(5)	0.43(5)	1.0
O4(8b)	0.2265(4)	0.2297(2)	0.1360(3)	0.36(3)	1.0
O5(4a)	0	0.1568(4)	0.3788(6)	0.57(6)	1.0
O6(8b)	0.7447(7)	0.3957(2)	0.3704(5)	0.38(4)	1.0
$LiSbO_3$,^{a} 2.73(10) wt %			CuO,^{b} 0.43(5) wt %		

$^a LiSbO_3$ is nonmagnetic and so does not effect our thermomag-
netic measurements.
^{b}The fraction of CuO ($T_N = 230$ K) in our sample is too small to
be detected in our measurements. At low T all of the Cu^{2+} spins
in CuO are frozen in an AFM ordered state; the absence of a spin
tail in the magnetic susceptibility [Fig. 2(a)] confirms this.

quality of our sample and confirms the absence of
any Cu site disorder. As has been noted elsewhere
[23,32–34], fitting χ^{-1} of FM-AFM chains to the Curie-
Weiss law is highly dependent on the fitting criteria. To
reduce the uncertainty in our analysis, the magnetic mo-
ment of the Cu^{2+} cations was fixed at $\mu_{eff} =
g_{av}\sqrt{S(S+1)}$. The average g factor $g_{av} = 2.10$ was deter-
mined by electron paramagnetic resonance measurements
at 4 K by using a Bruker K-band spectrometer and allows
us to experimentally determine $\mu_{eff} = 1.82\mu_B$ per formula
unit. A representative fit of the high T inverse susceptibility
χ^{-1} to the Curie-Weiss law, $\chi - \chi_0 = C/(T - \theta)$, for
$420 < T < 600$ K is inset in Fig. 2(a). While not unique
due to the ambiguity in defining χ_0, the value obtained
$\theta = 25(1)$ K is as would be expected for dominant FM
interactions.

Isothermal magnetization measurements up to 16 T in-
dicate proximity to a FM phase [Fig. 2(b)]. For $T < T_m$, the
magnetization has an "S" shape curvature associated with
an increase in the uniform FM component. At 2 K the
magnetization approaches saturation in the limiting 16 T
field. $dM/d(\mu_0 H)$ shows a maximum when $T < T_m$ indi-
cating an orientation-averaged saturation field $\mu_0\langle H_s\rangle =
12$ T in the low temperature limit. Our measurements
clearly indicate that 3D ordering is absent in $LiCuSbO_4$
down to 0.1 K in zero field. The low saturation field
$\mu_0\langle H_s\rangle = 12$ T is a further indication of very weak inter-
chain interactions [35].

Specific heat, C_p, measurements were performed on a
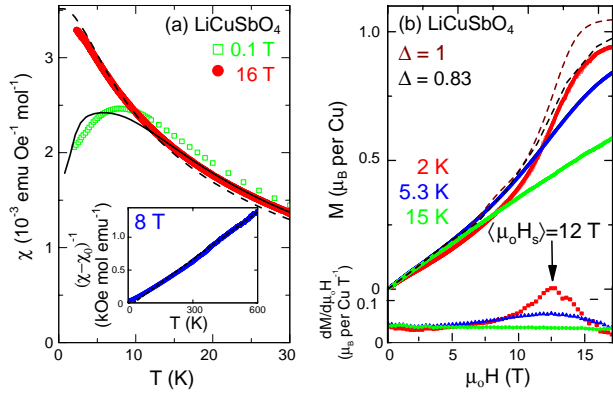Quantum Design physical properties measurement system.

FIG. 2 (color online). (a) Zero-field-cooled and field-cooled magnetic susceptibility of LiCuSbO$_4$ in a 0.1 and 16 T measuring field. The calculated susceptibilities for a 16-spin anisotropic frustrated chain model $\alpha = -0.45$, $J_1 = -75$ K, $\Delta = 0.83$, and $g_{av} = 2.10$ are shown in a 0.1 (solid line) and 16 T (dashed line) field. The high temperature inverse magnetic susceptibility in 8 T and the fit to the Curie-Weiss law ($\chi_0 = 7.36 \times 10^{-5}$ emu Oe^{-1} mol^{-1}) are inset. (b) Isothermal magnetization of LiCuSbO$_4$ and corresponding predictions for the frustrated chain model. At 2 K an isotropic (brown line) 24-spin system, $\alpha = -0.45$, $J_1 = -68$ K, is shown in addition to the anisotropic (black line) model. $dM/d\mu_0H$ is plotted below; for $T < T_m$, a clear maximum at $\mu_0H \sim 12$ T is observed.

To improve thermal conductivity, pellets of LiCuSbO$_4$ mixed with silver were used for our measurements. The C_p with the contribution from the silver powder [36] deducted is shown in Figs. 3(a)–3(c). In 0 T a broad maximum in C_p characteristic of the onset of SRO is observed for $T \sim 7.0$ K; this corresponds to a maximum in C_p/T at 4.3 K. With increasing field, the peak shifts to lower temperature, until at 10 T it is completely suppressed [Figs. 3(b) and 3(c)]. The lattice contribution to the C_p was modeled by using the Debye law ($\theta_D = 410$ K), and the magnetic entropy $\Delta S = \int C_p/T dT$ was extracted ($T > 0.1$ K) [Fig. 3(a), inset]. At high temperatures, ΔS measured in zero and an applied field converges, and at 50 K the 0 T measurement approaches the expected value ($R \ln 2$). At lower temperatures, $T < 2$ K, a second anomaly, $T \sim 0.6$ K, enhanced on application of a field, is observed for $\mu_0H \lesssim 13$ T. One possible origin for this anomaly is a multipolar transition as predicted theoretically for $H \sim H_s$ [4–6,8,9]. However, interpretation of high-field measurements in LiCuSbO$_4$ are complicated not only by the spherical averaging inherent to a powder sample but also because the alternating tilts of the easy axis of the CuO$_6$ octahedra results in an effective staggered field for all field orientations except $H\|a$. This can open a gap and preclude a phase transition [37]. Indeed, the broad nature of the peak in the C_p/T indicates a crossover rather than a phase transition. Single crystal experiments and more detailed theoretical work are needed to establish
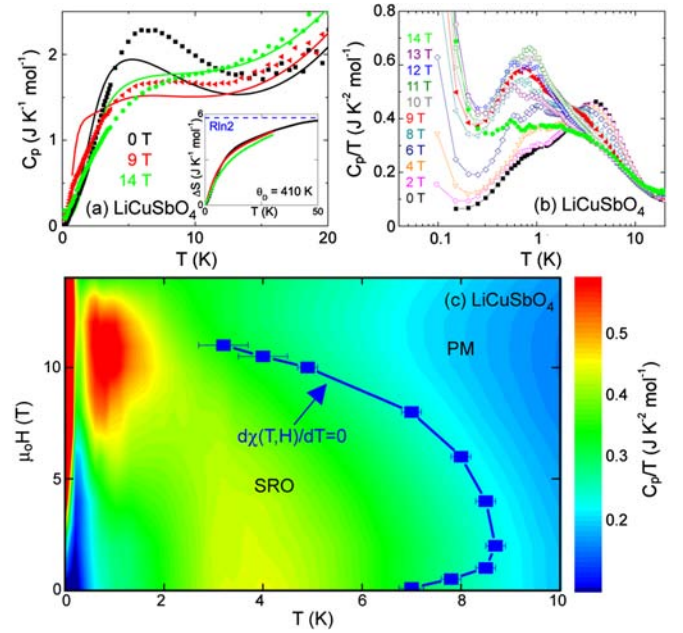

FIG. 3 (color online). (a) C_p as a function of field and temperature for selected fields. The lines indicate fits to the 16-spin anisotropic frustrated chain model, $\alpha = -0.45$, $J_1 = -75$ K, $\Delta = 0.83$, and $g_{av} = 2.10$ in a 0 (black line), 9 (red line), and 16 T (green line) applied field. The magnetic entropy $\Delta S = \int C_p/T dT$ integrated from 0.1 K is inset. (b) C_p/T as a function of temperature plotted on a logarithmic scale. (c) Contour plot of C_p/T as a function of field and temperature for LiCuSbO$_4$. The SRO transition as indicated by magnetic susceptibility (squares) is presented as a function of magnetic field and temperature.

the nature of the high-field phase suggested by the powder measurements.

To determine the relevant spin Hamiltonian, exact diagonalization (ED) of up to 20-spin rings was used to simultaneously model the magnetic susceptibility, isothermal magnetization, and specific heat [38]. Almost the complete temperature (2–300 K) and field (0–16 T) range of our thermomagnetic measurements was used to refine the ED model. As a generic first approximation to FM-AFM spin-$\frac{1}{2}$ chains [4,12,39], the model neglects g-tensor anisotropy and dipolar, hyperfine, and interchain interactions between spins. To reduce the number of parameters, an average g factor $g_{av} = 2.10$ determined by electron paramagnetic resonance was used. Initially, the magnetic properties were modeled with an isotropic chain, $\Delta = 1$. With $\alpha = -0.45$ and $J_1 = -68$ K, a good description of the thermodynamic data is obtained, though the high-field magnetization is overestimated [Fig. 2(b)]. To account for this, we included easy-plane anisotropy for the nearest-neighbor interactions, for simplicity leaving the next-nearest-neighbor interactions isotropic. We also neglect the more subtle effects of small deviations from an ideal square planar geometry. The model with $J_1 = -75$ K, $\alpha = -0.45$, and $\Delta = 0.83$ for 16 spins
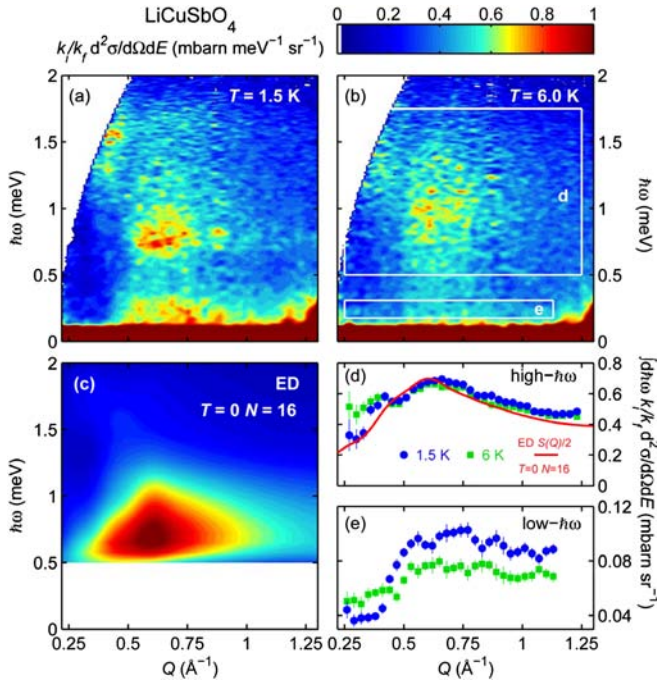
FIG. 4 (color online). (a) Low temperature inelastic neutron scattering data at $T = 1.5$ K and (b) $T = 6.0$ K. (c) Calculation of $S(Q, \omega)$ in absolute units for a spin-16 chain at $T = 0$ K using ED with $\alpha = -0.45$, $J_1 = -75$ K, and $\Delta = 0.83$. (d) Momentum-transfer dependence of the higher-energy signal, $0.50 < \hbar\omega < 1.75$ meV, and (e) quasielastic signal, $0.18 < \hbar\omega < 0.31$ meV. The color scale is in absolute units and consistent for frames (a)–(c). The intensity of the red solid line in (e) was rescaled by a factor of $1/2$ to compare with experimental results.

correctly reproduces the isothermal magnetization at 2 K [Fig. 2(b)]. This dramatic improvement in the fit to the isothermal magnetization when $\Delta = 0.83$ is due to a range of critical fields for a spherically averaged anisotropic model. Δ is of similar magnitude to that expected for Jahn-Teller distorted Cu^{2+}, $\Delta \sim 0.9$ [4]. The presence of two distinct Cu-Cu exchange pathways allows for a more complex J_1, J_1', J_2 exchange model; a 10% modulation of J_1 has no significant effect on the predicted properties. Given the insensitivity of the model to variation in J_1, we have not considered additional exchange interactions.

To explore the nature of the magnetic excitations at 0 T and test the magnetic exchange model inferred from the thermomagnetic measurements, inelastic neutron scattering on a powder sample of $^7LiCuSbO_4$ was carried out on the IN6 cold neutron time-of-flight time-focusing spectrometer at the Institut Laue-Langevin. The powder-averaged dynamical structure factor $S(Q, \omega)$ measured at $T = 1.5$ K and $T = 6.0$ K [Figs. 4(a) and 4(b)] displays intensity at low momentum transfer which can be unambiguously associated with magnetic excitations. For $T = 1.5$ K, the spectrum appears to be gapless within the 70 μeV elastic energy resolution of the instrument, and most of

the intensity is observed below 1.8 meV; no higher-energy intensity is detected below the maximal energy transfer accessible with $E_i = 3.12$ meV ($\lambda = 5.12$ Å). Comparing the 1.5 and 6 K spectra reveals that a magnetic quasielastic signal $\hbar\omega < 0.30$ meV develops at low temperature. As a function of momentum transfer, this signal is most intense for $Q = 0.52(1)$ Å^{-1} [Fig. 4(d)]. This corresponds to $Q = 0.475(9)\pi/a$ and is consistent with short-ranged incommensurate correlations in a frustrated spin chain with $\alpha = -0.45$ [39]. Remarkably, given the exchange parameters extracted from thermodynamic data, half of the magnetic scattering is found for $0.7 \leq \hbar\omega \leq 2.0$ meV [Figs. 4(b) and 4(e)]. The spectral maximum $\hbar\omega \sim 0.7$ meV is consistent with the 4.3 K maximum in the zero-field specific heat. To rigorously test the simplified spin Hamiltonian, we calculated the spherically averaged [40,41] dynamic response function $S(Q, \omega)$ with the parameters extracted from the thermodynamic data ($N = 16$, $J_1 = -75$ K, $\alpha = -0.45$, and $\Delta = 0.83$). The result [Fig. 4(e)] is remarkably consistent with the measured data given the absence of adjustable parameters [42].

$LiCuSbO_4$ is a novel crystalline quantum magnet with no 3D zero-field phase transition down to $T = 100$ mK. Using a combination of structural refinement, bulk magnetic properties, ED, and inelastic neutron scattering, we show that these unusual properties result from spin-$\frac{1}{2}$ chains with frustrated FM-AFM interactions ($\alpha = -0.45$). The extremely low and experimentally accessible saturation field of 12 T makes $LiCuSbO_4$ an ideal material in which to explore, in its entirety, the rich 1D physics predicted for frustrated spin-$\frac{1}{2}$ chains near quantum criticality.

*Corresponding author.
sed33@cam.ac.uk

[1] S.-L. Drechsler, J. Richter, A. A. Gippius, A. Vasiliev, A. A. Bush, A. S. Moskvin, J. Málek, Y. Prots, W. Schnelle, and H. Rosner, Europhys. Lett. **73**, 83 (2006).
[2] M. Hartel, J. Richter, D. Ihle, and S.-L. Drechsler, Phys. Rev. B **78**, 174412 (2008).
[3] H. T. Lu, Y. J. Wang, S. Qin, and T. Xiang, Phys. Rev. B **74**, 134425 (2006).
[4] S. Furukawa, M. Sato, and S. Onoda, Phys. Rev. Lett. **105**, 257205 (2010).

[5] J. Sudan, A. Luscher, and A. M. Lauchli, Phys. Rev. B **80**, 140402(R) (2009).

[6] T. Hikihara, L. Kecke, T. Momoi, and A. Furusaki, Phys. Rev. B **78**, 144404 (2008).

[7] A. V. Chubukov, Phys. Rev. B **44**, 4693 (1991).

[8] F. Heidrich-Meisner, I. P. McCulloch, and A. K. Kolezhuk, Phys. Rev. B **80**, 144417 (2009).

[9] M. E. Zhitomirsky and H. Tsunetsugu, Europhys. Lett. **92**, 37 001 (2010).

[10] S.-L. Drechsler *et al.*, Phys. Rev. Lett. **98**, 077202 (2007).

[11] M. Enderle *et al.*, Europhys. Lett. **70**, 237 (2005).

[12] M. Hase, H. Kuroe, K. Ozawa, O. Suzuki, H. Kitazawa, G. Kido, and T. Sekine, Phys. Rev. B **70**, 104426 (2004).

[13] M. Hase, K. Ozawa, O. Suzuki, H. Kitazawa, G. Kido, H. Kuroe, and T. Sekine, J. Appl. Phys. **97**, 10B303 (2005).

[14] M. Mourigal, M. Enderle, R. K. Kremer, J. M. Law, and B. Fåk, Phys. Rev. B **83**, 100409(R) (2011).

[15] M. Matsuda and K. Katsumata, J. Magn. Magn. Mater. **140**, 1671 (1995).

[16] M. Hase, I. Terasaki, and K. Uchinokura, Phys. Rev. Lett. **70**, 3651 (1993).

[17] W. E. A. Lorenz *et al.*, Europhys. Lett. **88**, 37 002 (2009).

[18] H. P. Bader and R. Schilling, Phys. Rev. B **19**, 3556 (1979).

[19] T. Hamada, J. Kane, S. Nakagawa, and Y. Natsume, J. Phys. Soc. Jpn. **57**, 1891 (1988).

[20] J. Sirker, V. Y. Krivnov, D. V. Dmitriev, A. Herzog, O. Janson, S. Nishimoto, S.-L. Drechsler, and J. Richter, Phys. Rev. B **84**, 144403 (2011).

[21] S. Park, Y. J. Choi, C. L. Zhang, and S-W. Cheong, Phys. Rev. Lett. **98**, 057601 (2007).

[22] S. Seki, Y. Yamasaki, M. Soda, M. Matsuura, K. Hirota, and Y. Tokura, Phys. Rev. Lett. **100**, 127201 (2008).

[23] M. Enderle, B. Fåk, H.-J. Mikeska, R. K. Kremer, A. Prokofiev, and W. Assmus, Phys. Rev. Lett. **104**, 237207 (2010).

[24] H. T. Lu, Y. J. Wang, S. Qin, and T. Xiang, Phys. Rev. B **74**, 134425 (2006).

[25] LiCuSbO$_4$ was prepared from a stoichiometric mixture of predried Li$_2$CO$_3$, CuO, and Sb$_2$O$_5$. Pellets were initially fired at 700 °C for 12 h, followed by a 24 h firing at 1000 °C. The progress of the reaction was monitored by using a Bruker D8 Focus x-ray diffractometer operating with Cu$K\alpha$ radiation and a graphite diffracted beam monochromator.

[26] Indexing of the powder pattern of LiCuSbO$_4$ using DICVOL06 [27] indicated a C-centered orthorhombic cell.

[27] D. Louer and A. Boultif, Z. Kristallogr. Suppl. **26**, 191 (2007).

[28] J. Choisnet, M. Hervieu, B. Raveau, and P. Tarte, J. Solid State Chem. **40**, 344 (1981).

[29] H. M. Rietveld, J. Appl. Crystallogr. **2**, 65 (1969).

[30] Room temperature measurements were taken with $\lambda =$ 1.5403 Å with a Cu(311) monochromator. The sample contained natural abundance Li, and an absorption correction was applied. Within the resolution of our diffraction measurements, $\pm 1\%$, Cu^{2+} is fully ordered on the 1D chains. To best account for the scattering density, a splitting of both the Li sites was included in the structural model. This disorder is within the *ab* plane, i.e., in the Li-Sb sheets, and reflects a mismatch in the size of the interstitial site and the Li$^+$ ions.

[31] J. Rodríguez-Carvajal, Physica (Amsterdam) **192B**, 55 (1993).

[32] S.-L. Drechsler *et al.*, arXiv:1006.5070.

[33] M. Enderle, B. Fåk, H.-J. Mikeska, and R. K. Kremer, arXiv:1009.1564.

[34] H.-J. Koo, C. Lee, M.-H. Whangbo, G. J. McIntyre, and R. K. Kremer, Inorg. Chem. **50**, 3582 (2011).

[35] S. Nishimoto, S.-L. Drechsler, R. O. Kuzian, J. van den Brink, J. Richter, W. E. A. Lorenz, Y. Skourski, R. Klingeler, and B. Büchner, Phys. Rev. Lett. **107**, 097201 (2011).

[36] D. R. Smith and F. R. Fickett, J. Res. Natl. Inst. Stand. Technol. **100**, 119 (1995).

[37] D. C. Dender, P. R. Hammar, D. H. Reich, C. Broholm, and G. Aeppli, Phys. Rev. Lett. **79**, 1750 (1997).

[38] The ED method has limitations due to finite size effects. For 16 spins this restricts accurate modeling to $T > 6$ K.

[39] J. Sirker, Phys. Rev. B **81**, 014419 (2010).

[40] P. R. Hammar, D. H. Reich, C. Broholm, and F. Trouw, Phys. Rev. B **57**, 7846 (1998).

[41] M. B. Stone, D. H. Reich, C. Broholm, K. Lefmann, C. Rischel, C. P. Landee, and M. M. Turnbull, Phys. Rev. Lett. **91**, 037205 (2003).

[42] A. P. Ramirez, C. L. Broholm, R. J. Cava, and G. R. Kowach, Physica (Amsterdam) **280B**, 290 (2000).